

seems plausible to assume that they are in fact the same. It must be remarked however that there is an appreciable discrepancy in energy between our value of 30.81 ± 0.03 kev and that of 30.0 kev reported by Scharff-Goldhaber *et al.*, and this assumption could be incorrect.

The intensities which were obtained by the method of Mladjenovic and Slätis⁵ from a densitometer trace are also given in Table II. The curve of efficiency for detection against gamma-ray energy is very steep in this region, so that these results are subject to greater errors than in the higher energy region. Nevertheless they should not be too bad for close-lying lines; the ratio M_1/M_3 might be expected to be more accurate than that for L_1/L_3 . Comparison between the observed and theoretical¹⁶ L subshell ratios for $M2$, $M3$, and $M4$ transitions clearly establishes the transition as $M3$. If this is so, the theoretical L -shell conversion coefficient should be 2.5×10^5 . Allowing a factor of 0.3 for the M , N , etc. shells this gives a total conversion coefficient of 3.3×10^5 . Thus if we take the half-life of the transition to be 5.7 hours, as given by Scharff-Goldhaber *et al.*,⁴ the gamma-ray half-life is 6.8×10^9 seconds. The half-life calculated from the single-particle formula is

1.4×10^5 sec so that the transition appears to be hindered by a factor of 5×10^4 .

The ground state of Os^{189} is known to have spin $3/2^{19}$ and this spin could be expected rather naturally from the Nilsson Scheme of levels in a deformed nuclear potential²⁰; the state would be the $3/2$ -[512] using the notation of paper II. The isomeric state would then be, equally naturally, the state $9/2$ -[505]. The $M3$ transition between these states is allowed according to the selection rules in the asymptotic quantum numbers. However, Os^{189} is getting rather far removed from the region of highly deformed nuclei where the asymptotic quantum numbers might be expected to be fairly good quantum numbers. The $3/2$ -state arises originally from the $f_{5/2}$ spherical state and the $9/2$ -state arises from the $h_{9/2}$ spherical state. An $M3$ transition between spherical states with these orbital angular momenta would be forbidden.

An $M3$ transition which is probably the same as that in Os^{189} but inverted occurs in Os^{191} .¹⁹ This transition has a similar large hindrance factor of 2×10^4 .

¹⁹ D. Strominger, J. M. Hollander, and G. T. Seaborg, *Revs. Modern Phys.* **30**, 585 (1958).

²⁰ S. G. Nilsson, *Kgl. Danske Videnskab. Selskab, Mat.-fys. Medd.* **29**, No. 16 (1955).

Reactions of Protons with Ni^{58} and Ni^{60}

SHELDON KAUFMAN

Frick Chemical Laboratories, Princeton University, Princeton, New Jersey

(Received October 9, 1959)

Excitation functions up to 19 Mev have been measured for the $\text{Ni}^{58}(p,2p)$, $\text{Ni}^{58}(p,pn)$, and $\text{Ni}^{58}(p,\alpha)$ reactions, and for the $\text{Ni}^{60}(p,\alpha)$ reaction up to 13 Mev. The ratio of the $(p,2p)$ cross section to the (p,pn) cross section is 3.5 at 19 Mev, and increases with decreasing energy. It is proposed that this excess of proton emission can be accounted for by nuclear evaporation theory, and a computer calculation of the excitation functions using this theory is described. The calculation reproduces the $(p,2p)$ and (p,pn) curves quite well, and gives evidence that the compound nucleus mechanism probably applies to these reactions. The calculated (p,α) curve does not agree with the experimental results as well.

I. INTRODUCTION

IT is commonly assumed that in nuclear reactions at low energies (less than about 30-Mev excitation energy) emission of charged particles from a compound nucleus is improbable except in the lightest elements, because of the Coulomb barrier. The observation¹⁻³ that many reactions in which protons or alpha particles were emitted had relatively large cross sections led to the rejection of a compound nucleus mechanism for such reactions. Instead, a direct interaction of the incident particle with a single nucleon (or alpha-

particle group) inside the nucleus was proposed, in order that most of the available energy be given to the emitted particle, rather than shared with the entire nucleus.

A large cross section for such a reaction is not necessarily evidence that a compound nucleus is not formed, however. There may be factors other than the Coulomb barrier affecting the reaction which will tend to enhance the probability of emitting a charged particle. For example, the threshold energy may be considerably lower for such a reaction than for one involving neutron emission. This will provide the excess energy needed by the particle to overcome the Coulomb barrier. Another factor which can be important is the relative level densities of the residual nuclei. It is

¹ S. N. Ghoshal, *Phys. Rev.* **80**, 939 (1950).

² E. B. Paul and R. L. Clarke, *Can. J. Phys.* **31**, 267 (1953).

³ Cohen, Newman, and Handley, *Phys. Rev.* **99**, 723 (1955).

difficult to predict the effect of these factors without carrying out the appropriate calculations.

A striking example of an excess of charged-particle emission is the case of Ni^{58} bombarded with protons.³ At an energy of 21.5 Mev, the ratio of cross sections of the $(p,2p)$ to the (p,pn) reaction was measured as 2.8. The threshold of the former reaction is 4 Mev less than that of the latter. In addition, there is good reason to believe that the Ni^{57} nucleus has a lower level density than the Co^{57} nucleus at the same excitation energy, because of the closed shell of protons in the former. Both of these would increase the probability of proton emission, and would give an explanation of the large $(p,2p)$ cross section. A cross section measurement at a single energy does not usually provide an adequate comparison with theory. Therefore, the cross sections of these reactions were measured as a function of proton energy up to 19 Mev, and the results compared with the predictions of the compound nucleus-statistical theory of nuclear reactions. In addition, the (p,α) reactions of Ni^{58} and Ni^{60} were measured.

II. EXPERIMENTAL PROCEDURE AND RESULTS

Targets were bombarded in the external proton beam of the Princeton University cyclotron, which has a maximum energy of 19 Mev. Two kinds of targets were used: 0.35-mil nickel foil of natural isotopic composition, and Ni^{58} enriched to 99.6%,⁴ which was electroplated onto 0.5-mil platinum foil for the bombardments. Four bombardments, two with each kind of target, were made. The usual stacked-foil technique of measuring excitation functions was used, with nickel foils interspersed with aluminum foils to degrade the proton energy. The protons were magnetically focussed, and collimated by a pair of graphite blocks with $\frac{1}{4}$ -inch apertures. The mean energy of the protons was measured to 0.3% accuracy by determining their range in aluminum.⁵ The beam current was measured with a Faraday cup connected to a precision condenser, and the voltage across the condenser read on a calibrated quadrant electrometer. The beam current could be measured only when the foil stack was not being bombarded, because the stack scattered a large fraction of the protons away from the Faraday cup. The targets were withdrawn from the beam periodically in order to measure the current, and the beam was monitored during the course of a bombardment to note any changes in the relative intensity. The integrated number of protons over the entire bombardment could then be calculated.

The mean energy of the protons in each foil in the stack was calculated by using the theoretical expression for the rate of energy loss of charged particles passing

through matter,⁶ with recently determined values of I/Z , the ratio of the mean ionization potential to the atomic number.^{7,8} The spread of energies about this mean was calculated from the initial energy spread of the beam, 0.25 Mev,⁵ and the additional spread due to straggling in the absorbers.⁶

After the bombardment the targets were dissolved in HCl, to which $\text{Co}(\text{NO}_3)_2$ carrier had been added. The surface layer of the platinum supporting foil was also dissolved in the case of the enriched Ni^{58} targets, although most of the platinum remained inert. The solution was passed through an ion-exchange column of Dowex-1,⁹ which served to separate Ni from Co, Cu, Pt, and Au.¹⁰ The Co was eluted selectively from the column, and was subjected to further chemical purification, after which it was precipitated and mounted for counting. The Ni fractions were set aside to allow Ni^{57} to decay completely to Co^{57} , which was then separated as in the Co fractions, and counted.

The Co samples were counted with an end-window GM counter and an end-window beta proportional counter of the flow type. Both counters used helium as a counting gas, in order to have a low counting efficiency for low-energy x rays. Co^{55} was present in all samples, as shown by the initial 18-hour half-life. The counting efficiency of the counters for the Co^{55} beta rays was determined by means of a number of Co^{55} standards of different thickness. The disintegration rates of the standards were measured by a γ - γ coincidence technique, using the annihilation radiation.¹¹ The disintegration rates obtained must be corrected for the fraction of Co^{55} nuclei which decay by beta emission, which was taken as 0.65.^{12,13}

The Co^{57} in the Co samples and in the samples from the Ni^{57} decay was counted by detecting the 123-kev and 137-kev gamma rays with a $1\frac{1}{2} \times 1$ -inch NaI crystal and a single-channel pulse-height analyzer. A standard Co^{57} source was calibrated by counting its gamma rays with a 4π -geometry scintillation counter¹⁴ to determine its disintegration rate, and this was used to determine the efficiency of the particular counting geometry and channel width used for the samples. No gamma rays above 200 kev could be detected in any

⁶ H. A. Bethe and J. Ashkin, in *Experimental Nuclear Physics*, edited by E. Segrè (John Wiley and Sons, Inc., New York, 1953), Vol. 1.

⁷ Bichsel, Mozley, and Aron, *Phys. Rev.* **105**, 1788 (1957).

⁸ V. C. Burkig and K. R. MacKenzie, *Phys. Rev.* **106**, 848 (1957).

⁹ Manufactured by Dow Chemical Company, Midland, Michigan.

¹⁰ K. A. Kraus and G. E. Moore, *J. Am. Chem. Soc.* **75**, 1460 (1953).

¹¹ The coincidence counting was done by Mr. L. Remsberg, of the Nevis Cyclotron Laboratories, Columbia University.

¹² *Nuclear Level Schemes, A=40—A=92*, compiled by Way, King, McGinnis, and van Lieshout, Atomic Energy Commission Report TID-5300 (U. S. Government Printing Office, Washington, D. C., 1955).

¹³ Mukerji, Dubey, and Malik, *Phys. Rev.* **111**, 1319 (1958).

¹⁴ A. E. Metzger and J. M. Miller, *Phys. Rev.* **113**, 1125 (1959).

⁴ Obtained from the Stable Isotopes Division, Oak Ridge National Laboratory.

⁵ G. Schrank, *Rev. Sci. Instr.* **26**, 677 (1955).

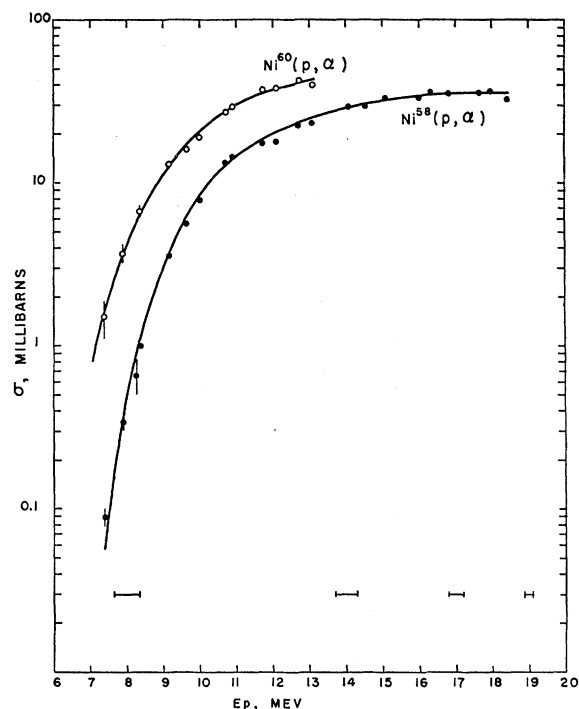


FIG. 1. Excitation functions for the reactions $\text{Ni}^{58}(p, \alpha)\text{Co}^{55}$ and $\text{Ni}^{60}(p, \alpha)\text{Co}^{57}$. Vertical lines indicate the error due to counting, horizontal lines at the bottom indicate the spread in beam energy at different energies in the foil stack. Smooth curves have been drawn through the experimental points.

of the samples, showing that they were free of the other long-lived Co activities, Co^{56} , Co^{58} , and Co^{60} .

The chemical yield of each sample was measured after it was counted by colorimetric analysis, using the Nitroso-R Salt method.¹⁵ Nickel was precipitated and weighed as the dimethylglyoxime derivative.

The cross sections were calculated using the formulas derived by Rudstam¹⁶ for a varying beam current during a bombardment. The resulting excitation functions are shown in Figs. 1 and 2. The vertical lines indicate the standard deviation due to counting only. The horizontal lines indicate the energy spread in the targets due to the initial energy spread and to straggling. The absolute cross sections are accurate to about 10%, mainly due to variations in the beam current during bombardment. The consistency of points from different bombardments is about 10%. An additional uncertainty of about 10% in the absolute cross section of the $\text{Ni}^{58}(p, \alpha)\text{Co}^{55}$ reaction is due to the difficulties present in beta counting and to the uncertain decay scheme of Co^{55} .

Co^{57} is produced by two reactions in natural nickel, $\text{Ni}^{58}(p, 2p)$ and $\text{Ni}^{60}(p, \alpha)$. Below 13 Mev, where the $\text{Ni}^{58}(p, 2p)$ reaction has a small cross section, its contribution may be subtracted from the total Co^{57} activity, and the $\text{Ni}^{60}(p, \alpha)$ cross section determined.

¹⁵ E. B. Sandell, *Colorimetric Determination of Traces of Metals* (Interscience Publishers, Inc., New York, 1950).

¹⁶ G. Rudstam, thesis, Uppsala, 1956 (unpublished).

In Figs. 1 and 2 smooth curves have been drawn through the experimental points in order to show the shape of the excitation functions more clearly. The curves are quite similar for the two (p, α) reactions. If the $\text{Ni}^{60}(p, \alpha)$ curve is shifted to higher energies by 1.2 Mev, which is the difference in Q of the two reactions, the curves become identical up to a cross section of about 20 mb, after which the $\text{Ni}^{60}(p, \alpha)$ curve rises faster, and so attains a higher peak cross section. The (p, α) cross section on Ni at 23 Mev has been measured¹⁷ by detecting the alpha particles; the value obtained was 93.5 mb, which is more than twice as high as the peak value of 36 mb at 16–18 Mev obtained in this work. This discrepancy is undoubtedly due to the difference in energy, and to the fact that $(p, \alpha n)$ and $(p, \alpha p)$ reactions are included in the counter experiment, but not in the radiochemical experiment.

The $\text{Ni}^{58}(p, 2p)$ cross section is higher than the (p, pn) cross section at all energies available, the ratio decreasing with increasing energy. The points at 21.5 Mev are from Cohen *et al.*³ The agreement with the trend of this work is good.

The ratio of Co^{57} produced to Ni^{57} produced has now been measured in a number of nuclear reactions.^{3, 18–20}

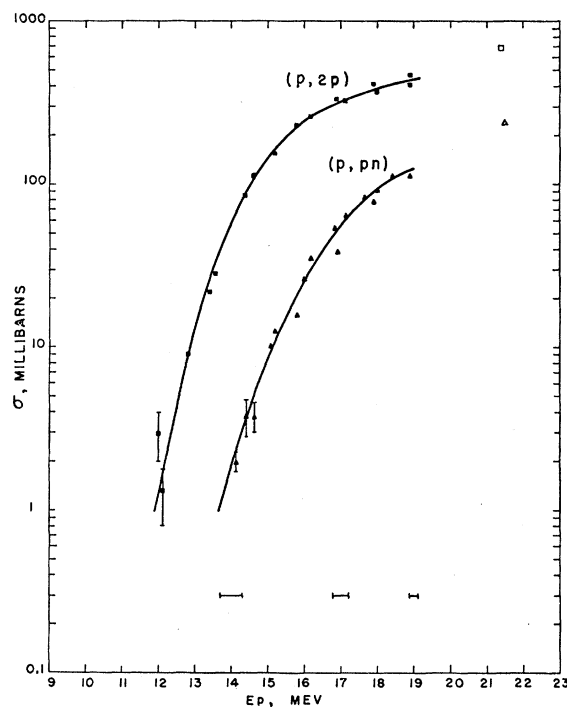


FIG. 2. Excitation functions for the reactions $\text{Ni}^{58}(p, 2p)\text{Co}^{57}$ and $\text{Ni}^{58}(p, pn)\text{Ni}^{57}$. See caption to Fig. 1.

¹⁷ C. B. Fulmer and B. L. Cohen, *Phys. Rev.* **112**, 1672 (1958).

¹⁸ J. M. Miller and F. S. Houck, *Bull. Am. Phys. Soc.* **4**, 60 (1957); F. S. Houck, thesis, Columbia University, New York, 1959 (unpublished).

¹⁹ K. H. Purser and E. W. Titterton, *Australian J. Phys.* **12**, 103 (1959).

²⁰ J. H. Carver and W. Turchinets, *Proc. Phys. Soc. (London)* **73**, 585 (1959).

A summary of the results obtained is presented in Table I. That this ratio is approximately constant for such different bombarding particles and energies is strong evidence that a Ni^{58} compound nucleus, whose decay to this isobaric pair is independent of its mode of formation, is involved. It has been suggested^{3,21} that a direct interaction mechanism, in which a proton is knocked out of the nucleus by the incident proton, which also escapes, could explain the high $(p,2p)$ cross section. It is difficult to see how such a process could be independent of the nature of the bombarding particles, as it is to a good approximation. The same objection applies to another suggestion,²¹ that the incident particle has a high probability of re-emission.

In view of the strong possibility that a compound nucleus mechanism is involved, it was decided to carry out a numerical computation of the excitation functions for the Ni^{58} reactions, using as few approximations as was consistent with reasonable computer time. The Princeton University IBM-650 digital computer was used for these computations, which are described in the next section.

III. THE EVAPORATION CALCULATION

A. Equations and Input Data

According to the compound nucleus theory, the nuclear reaction $A(p,xy)D$ is considered to take place in two steps: the formation of a compound nucleus $A+p \rightarrow B$, and its subsequent decay, $B \rightarrow C+x$, $C \rightarrow D+y$. The cross section for the reaction is given by

$$\sigma(p,xy) = \sigma_{pA}(\epsilon_p) G_{xy}(U), \quad (1)$$

where $\sigma_{pA}(\epsilon_p)$ is the cross section for protons of energy ϵ_p reacting with nucleus A to form the compound nucleus B with excitation energy U ; and $G_{xy}(U)$ is the probability that particle x will be emitted from B , followed by particle y being emitted from C . The absolute probability $G_{xy}(U)$ is expressed in terms of relative probabilities $F_i(U)$:

$$G_{xy}(U) = F_{xy}(U) / \sum_i F_i(U). \quad (2)$$

The summation is over all particles which can be

TABLE I. The ratio of the cross section for forming Co^{57} to that for forming Ni^{57} , using various targets and bombarding particles.

Reaction	Bombarding energy, Mev	$\sigma(\text{Co}^{57}) / \sigma(\text{Ni}^{57})$	Ref.
$\text{Ni}^{58}+p$	19	3.5	This work
$\text{Ni}^{58}+p$	21.5	2.8	3
$\text{Ni}^{58}+\alpha$	40	5.0	18
$\text{Fe}^{54}+\alpha$	30	4.0	18
$\text{Ni}^{58}+n$	14.1	4.5	19
$\text{Ni}^{58}+\gamma$	32	2.35	20

²¹ B. L. Cohen, Phys. Rev. **108**, 768 (1957).

emitted; at the relatively low energies under consideration only proton, neutron, alpha particle, deuteron, and gamma ray are included. The probability $F_{xy}(U)$ is given by the statistical theory of nuclear reactions²² as

$$F_{xy}(U) = g_x \int_0^{U-S_x-S_y} \epsilon_x \sigma_C(\epsilon_x) \times \omega_C(U-S_x-\epsilon_x-\delta_C) G_{Cy}(\epsilon_x) d\epsilon_x. \quad (3)$$

In this equation, S_x and S_y are separation energies of x from B and y from C , respectively; ϵ_x is the kinetic energy of x ; $\sigma_C(\epsilon_x)$ is the cross section for the reaction $C+x \rightarrow B$; $\omega_C(E)$ is the level density of C at excitation energy E ; G_{Cy} is the probability that C will emit particle y ; and g_x is a statistical weighting factor for particle x , given by

$$g_x = (2I_x + 1) M_x / 2M_p,$$

where I_x is the spin and M_x the mass of particle x , and M_p the mass of the proton.

G_{Cy} is given by equations similar to Eqs. (2) and (3):

$$G_{Cy}(\epsilon_x) = F_{Cy}(\epsilon_x) / \sum_j F_{Cj}(\epsilon_x), \quad (4)$$

$$F_{Cy}(\epsilon_x) = g_y \int_0^{U-S_x-S_y-\epsilon_x} \epsilon_y \sigma_D(\epsilon_y) \times \omega_D(U-S_x-S_y-\epsilon_x-\epsilon_y-\delta_D) d\epsilon_y. \quad (5)$$

Equations (3) and (5) do not apply to gamma ray emission. This is important only below the threshold for neutron emission and when the charged particle competing with the gamma ray has a kinetic energy much less than the Coulomb barrier. Values of F_γ were determined from experimental data on (n,γ) and $(n, \text{nonelastic})$ cross sections for nuclei in the Ni region.²³ For neutron energies of 1–2 Mev, F_γ was approximately 0.1, which was the value used in the calculations. The value of F_p exceeds this when the proton energy is about 2 Mev, in agreement with the findings of Meadows.²⁴

Previous evaporation calculations have used approximate expressions for σ , the cross section for the inverse reaction, for charged particles. These approximations usually have the effect of predicting too low a cross section for charged particle emission near the threshold, since they do not properly take into account the penetration of the Coulomb barrier. Shapiro²⁵ has made extensive calculations of the cross section for compound nucleus formation by different charged particles as a function of energy. The appropriate values from this table were fed into the memory of the computer, and an interpolation program was used to compute the cross section at any energy. Above the range of Shapiro's

²² J. M. Blatt and V. F. Weisskopf, *Theoretical Nuclear Physics* (John Wiley and Sons, Inc., New York, 1952), Chap. VIII.

²³ D. J. Hughes and R. B. Schwartz, *Neutron Cross Sections*, Atomic Energy Commission Report BNL-325 (U. S. Government Printing Office, Washington, D. C., 1958), 2nd ed.

²⁴ J. W. Meadows, Phys. Rev. **98**, 744 (1955).

²⁵ M. M. Shapiro, Phys. Rev. **90**, 171 (1953), Table IV.

TABLE II. Coulomb barriers used in the calculation.

Nucleus	Coulomb barrier, Mev		Alpha particle
	Proton	Deuteron	
$^{28}\text{Ni}^{58}$	6.96		
$^{28}\text{Ni}^{57}$	7.00	5.77	
$^{27}\text{Co}^{57}$	6.74		
$^{27}\text{Co}^{55}$			10.3
$^{26}\text{Fe}^{54}$	6.61		

calculations, the asymptotic expression

$$\sigma(\epsilon) = \pi(R + \lambda)^2 [1 - BR/\epsilon(R + \lambda)] \quad (6)$$

was used, where R is the nuclear radius, λ is the reduced wavelength of the particle, and B is the Coulomb barrier. This use of a table of numbers required the integrations to be carried out numerically. The neutron cross section was taken from the curves given by Blatt and Weisskopf²⁶; to a good approximation it is independent of energy above 1 Mev, and the value used in the calculation was $1.3\pi R^2$.

The level density is given by the statistical model as

$$\omega(E) = C \exp[2(aE)^{\frac{1}{2}}], \quad (7)$$

where E is the excitation energy and C and a are constants. Hurwitz and Bethe²⁷ have suggested that the level density should be calculated from a characteristic level above the ground state, to take account of the pairing energy of an even number of protons or neutrons. If the pairing energy of the nucleus is δ , then the level density is

$$\omega(E) = C \exp\{2[a(E - \delta)]^{\frac{1}{2}}\}, \quad (8)$$

where $\delta = 0$ for odd-odd nuclei and $\delta \geq 0$ for other types. Cameron²⁸ has compiled a table of pairing energies used in his semiempirical mass formula, and these values were used in this calculation. The effect of a nuclear closed shell on the level density was taken into account by an additional δ term in Eq. (8). Since Cameron's table does not take closed shells into account, this additional term was selected to give the best fit

TABLE III. Threshold energies of the reactions considered.^a

Reaction	Threshold energy, Q , Mev
$\text{Ni}^{58}(p, p)\text{Ni}^{58}$	0
$\text{Ni}^{58}(p, n)\text{Cu}^{58}$	- 9.2 ^b
$\text{Ni}^{58}(p, 2p)\text{Co}^{57}$	- 7.78
$\text{Ni}^{58}(p, pn)\text{Ni}^{57}$	- 11.80
$\text{Ni}^{58}(p, d)\text{Ni}^{57}$	- 9.57
$\text{Ni}^{58}(p, 2n)\text{Cu}^{57}$	- 21.4 ^c
$\text{Ni}^{58}(p, \alpha)\text{Co}^{55}$	- 1.23
$\text{Ni}^{58}(p, \alpha p)\text{Fe}^{54}$	- 6.28
$\text{Ni}^{58}(p, \alpha n)\text{Co}^{54}$	- 15.97

^a Computed from the mass tables of Wapstra, except where noted.

^b Sutton, Hill, and Sherr, Bull. Am. Phys. Soc. **4**, 278 (1959).

^c A. G. W. Cameron, Chalk River Report CRP-690, 1957 (unpublished).

²⁶ See reference 22, p. 348.

²⁷ H. Hurwitz and H. A. Bethe, Phys. Rev. **81**, 898 (1951).

²⁸ A. G. W. Cameron, Can. J. Phys. **36**, 1040 (1958).

with experiment. A further correction to δ was found to be necessary in the case of Cu^{58} , in order to obtain a reasonable agreement with experiment. Dostrovsky *et al.*,²⁹ in their Monte Carlo evaporation calculations, included a "symmetry" term in δ , for nuclei with $Z = N$, which seem to have a lower level density than expected from pairing alone. Cu^{58} is in this class, with $Z = N = 29$, and a correction of 0.5 Mev was added to the δ for Cu^{58} and also Co^{54} , the other symmetric nucleus in the calculation. The values of δ used in the calculation are given in Table IV, with the shell and symmetry corrections that gave the best fit to the experimental data.

Equation (8) for the level density has the undesirable property of eliminating all levels between the ground state and the characteristic level, which would strongly affect the calculated cross section near the threshold. Since the level density in this region is small and probably constant, it would be desirable to set $\omega = C$ there. Weinberg and Blatt³⁰ have proposed a formula which allows this to happen in a smooth manner. Their

TABLE IV. Values of δ used in the calculation. δ_Z and δ_N are taken from Cameron's table, while the shell and symmetry terms are those that gave the best fit to experiment when added in.

Nucleus	δ_Z	δ_N	δ_{shell}	δ_{sym}	δ_{Total}
$^{29}\text{Cu}^{58}$	0	0	0	0.5	0.5
$^{28}\text{Ni}^{58}$	1.37	1.32	1.0	0	3.69
$^{28}\text{Ni}^{57}$	1.37	0	1.0	0	2.37
$^{27}\text{Co}^{57}$	0	1.32	0	0	1.32
$^{27}\text{Co}^{55}$	0	1.47	0.5	0	1.97
$^{27}\text{Co}^{54}$	0	0	0	0.5	0.5
$^{26}\text{Fe}^{54}$	1.45	1.47	0.5	0	3.42

expression is

$$\omega'(E) = C \exp[2(aE')^{\frac{1}{2}}],$$

$$E' = \frac{E - \delta}{1 - \exp[-a(E - \delta)]}. \quad (9)$$

Both Eq. (8) and Eq. (9) were used in the calculations, with results which will be described below.

The parameter a has been calculated on the basis of several models, and measured in a number of experiments.³¹ As in the work of Dostrovsky *et al.*,³¹ values of $a = A/10$ and $a = A/20$ were used at first, and then a was regarded as an adjustable parameter to be determined by comparison with experiment.

The values of the parameters used in the calculation are summarized in Tables II-IV. The barrier heights in Table II were calculated for a nuclear radius of $R = 1.5A^{\frac{1}{3}} \times 10^{-13}$ cm and a deuteron radius of 1.21×10^{-13} cm. The radius of interaction for the alpha particle chosen was that obtained from the elastic

²⁹ Dostrovsky, Fraenkel, and Friedlander, Phys. Rev. **116**, 683 (1959).

³⁰ I. G. Weinberg and J. M. Blatt, Am. J. Phys. **21**, 124 (1953).

³¹ Dostrovsky, Rabinowitz, and Bivins, Phys. Rev. **111**, 1659 (1958), discuss the values obtained.

scattering of alpha particles,³² $R = (1.414A^{1/3} + 2.190) \times 10^{-13}$ cm. The masses used in calculating the threshold energies are from Wapstra,³³ except where noted. The relationship between these energies and U is

$$U - S_x - S_y = E_p + Q(p, xy). \quad (10)$$

B. Results and Discussion

Some general features of the calculation will be discussed first, and then the results will be compared with experiment. The effect of using Eq. (8) or Eq. (9) for the level density was compared first. It was found that Eq. (8) resulted in calculated cross sections which were displaced from the experimental curves toward higher energies by several Mev, and which had a steeper rise in the initial portion. The calculations could be made to agree better with experiment by subtracting a fixed amount from each δ , making some of them negative. This is equivalent to redefining the position of the characteristic level, so that it lies below the ground state of some nuclei. Using Eq. (9) for the level density with positive values of δ gave curves in much better agreement with experiment near threshold; this level density formulation was therefore used in all subsequent calculations.

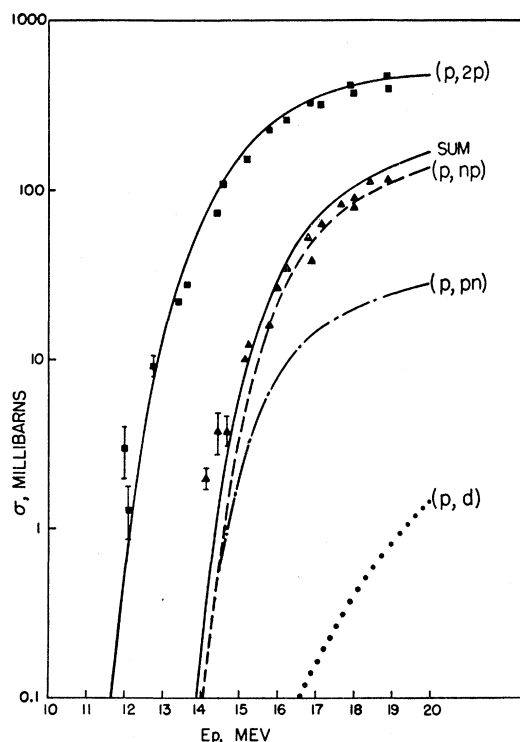


FIG. 3. Calculated excitation functions for $\text{Ni}^{58}(p, 2p)$, $\text{Ni}^{58}(p, np)$, $\text{Ni}^{58}(p, pn)$, and $\text{Ni}^{58}(p, d)$, using $a = 4.5$. The curve labeled "sum" is the sum of the three reactions producing Ni^{57} . The experimental points are given for comparison.

³² Kerlee, Blair, and Farwell, Phys. Rev. **107**, 1343 (1957).

³³ A. H. Wapstra, Physica **21**, 385 (1955).

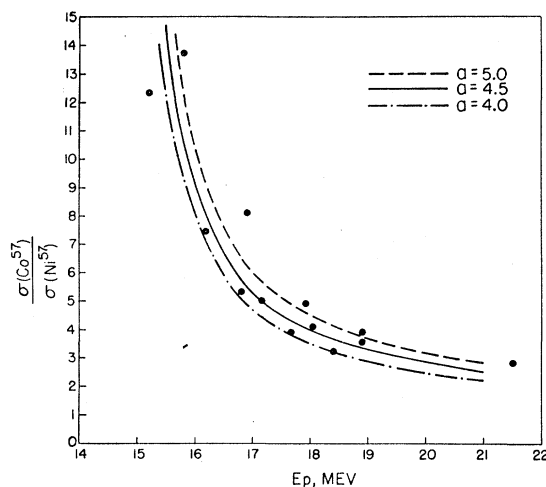


FIG. 4. Calculated ratio of the cross section for producing Co^{57} to that for producing Ni^{57} , using three values of a . The experimental points are given for comparison. The point at 21.5 Mev is from reference 3.

The value of the level density parameter a had an effect on both the shape of the curves and the size of the cross section. Lowering a , which is equivalent to raising the nuclear temperature for a given excitation energy, increased the (p, α) and (p, pn) cross sections, and decreased the $(p, 2p)$ cross section. The initial rise of the (p, α) and (p, pn) curves was steepened also. As pointed out by Dostrovsky *et al.*,³¹ decreasing a usually increases the emission probability of the "rarer" particles relative to neutrons. In this case, the neutron is itself "rarer" than the proton, hence the result above.

The exact values of δ used are not as important to the calculation as their relative magnitudes. Apart from shell effects, an even-even nucleus should have a δ of about twice that of an odd-even or even-odd nucleus, and an odd-odd nucleus a δ of zero. If the values of δ are changed, a change in a will often restore the original curves, or very nearly so. Thus the "best values" of the parameters reported below are not unique, but rather are representative of a range of possible values. On the other hand, this fact gives confidence that reproducing the experimental curves depends more on the general features of separation energies and relative magnitudes of δ , rather than on some special combination of numbers.

As an example of this, a decrease in the shell contribution to δ for 28 protons leaves the $(p, 2p)$ and (p, np) cross sections almost unchanged. This is because the former reaction must proceed through Ni^{58} as an intermediate nucleus, while the latter reaction ends in Ni^{57} ; if the δ for both nuclei is decreased, the two reactions both increase by almost the same amount.

The best fit to the experimental data was obtained using the values of δ listed in Table IV, and with $a = 4.5$. The computed curves for these values are compared with the experimental data in Figs. 3-5.

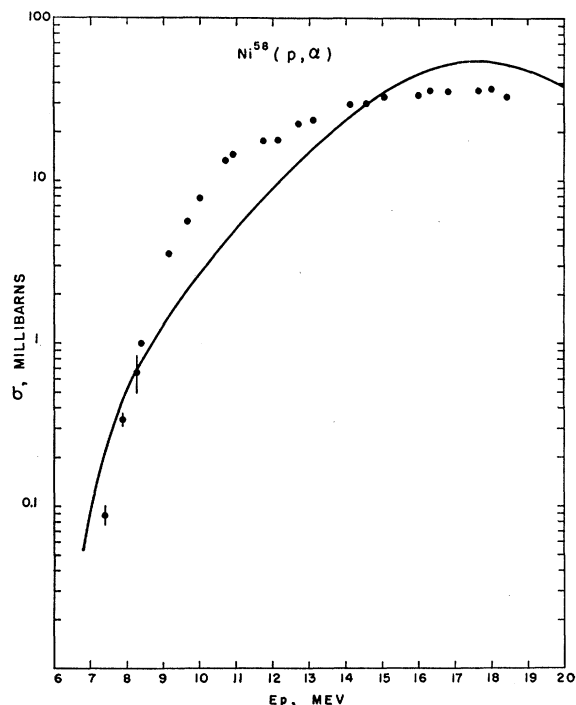


FIG. 5. Calculated excitation function for $\text{Ni}^{58}(p, \alpha)$, using $a=4.5$. The experimental points are given for comparison.

Figure 3 shows the $(p, 2p)$ cross section, and how the total (p, pn) cross section is made up of the sum of the three reactions which produce Ni^{57} . That the (p, np) cross section is much larger than the (p, pn) cross section can be understood as follows: Evaporation of a neutron from Cu^{69} is likely to leave the Cu^{58} nucleus with considerable excitation energy, since low-energy neutrons are not hindered by a Coulomb barrier. But the separation energy of a proton from the latter nucleus

is only 2.6 Mev, and since a proton need only compete with a gamma ray, a (p, np) reaction results if the Cu^{58} is left with more than about 5 Mev of excitation. On the other hand, when Cu^{69} evaporates a proton, the resulting Ni^{58} nucleus is likely to have a low excitation energy, since the proton must have enough energy to penetrate the Coulomb barrier efficiently. This favors proton emission from the Ni^{58} nucleus because of the 4 Mev lower separation energy of the proton. Thus, most (p, n) reactions are followed by proton emission, while very few (p, p) reactions are followed by neutron emission, and most of the Ni^{57} results from the (p, np) reaction.

Figure 4 shows the ratio of Co^{57} to Ni^{57} formed as a function of proton energy, and the computed curves for three different values of a . It is seen that a lower a favors more neutron emission relative to proton emission, as noted above. These curves enabled the choice of $a=4.5$ to be made.

Figure 5 shows the calculated curve and experimental points for the $\text{Ni}^{58}(p, \alpha)$ reaction. Although the threshold region and the peak cross section are in fair agreement with experiment, the calculated curve has a slower rise and a sharper peak than is found experimentally. Attempts to modify this shape by changing the parameters met with little success. If a is lowered sufficiently, the curve can be made to fit the points quite well below 12 Mev, but then the peak cross section is too high. Lowering δ for Co^{55} , or lowering the alpha-particle barrier produces much the same effect.

ACKNOWLEDGMENTS

The author would like to thank the Food Machinery and Chemical Corporation for funds for the purchase of equipment. He wishes to acknowledge several helpful discussions of the evaporation calculations with Dr. G. Friedlander and Dr. J. M. Miller.